

Direct observation of electric-quadrupolar order in UO_2

S. B. Wilkins,^{1,2} R. Caciuffo,¹ C. Detlefs,² J. Rebizant,¹ E. Colineau,¹ F. Wastin,¹ and G. H. Lander¹

¹European Commission, Joint Research Centre, Institute for Transuranium Elements, Postfach 2340, Karlsruhe D-76125, Germany

²European Synchrotron Radiation Facility, Boîte Postal 220, F-38043 Grenoble Cedex, France

(Received 23 August 2005; revised manuscript received 13 January 2006; published 17 February 2006)

We report direct experimental evidence for long-range antiferro ordering of the electric-quadrupole moments on the U ions. Resonant x-ray scattering experiments at the uranium M_4 absorption edge show a characteristic dependence in the integrated intensity upon rotation of the crystal around the scattering vector. Although quadrupolar order in uranium dioxide was advocated already in the 1960s, no experimental evidence for this phenomenon was provided until now. We conclude with a possible model to explain the phase diagram of the solid solutions of UO_2 and NpO_2 . We suggest that in the region $0.30 < x < 0.75$ of $\text{U}_{(1-x)}\text{Np}_x\text{O}_2$ neither the transverse nor the longitudinal quadrupole ordering can dominate, leading to frustration and only short-range ordering.

DOI: 10.1103/PhysRevB.73.060406

PACS number(s): 75.25.+z, 75.10.-b, 78.70.Ck

Uranium dioxide (fcc CaF_2 crystal structure with space group $Fm\bar{3}m$) is the most studied of any actinide material because of readily available single crystals and industrial applications. Since the 1950s, many important experiments have been performed to elucidate the nature of the low-temperature ground state of UO_2 . These include the determination of the magnetic structure below T_N ($=31$ K) and value of the magnetic moment,^{1,2} the strong softening of the c_{44} elastic constant starting at temperatures considerably above T_N ,³ the evidence for strong magnon-phonon coupling,⁴ the observation of an internal rearrangement of the oxygen atoms below T_N ,⁵ and evidence that the magnetic structure is of the $3\mathbf{k}$ variety.⁶ Further evidence supporting the noncollinear $3\mathbf{k}$ ordering was provided by neutron inelastic scattering,⁷ and NMR studies.⁸

In addition to the wealth of experimental data, important theories were developed, notably the work of Allen,^{9,10} Sasaki and Obata,¹¹ Siemann and Cooper,¹² and Solt and Erdős.¹³ Even in the last three years a number of theoretical papers have been published.¹⁴⁻¹⁷ To a lesser or greater extent, all these theories emphasize the importance of the interplay between the Jahn-Teller and quadrupolar interactions in UO_2 .

Experimentally, however, no direct evidence for the ordering of electric quadrupole moments below T_N has been presented. This paper provides that key evidence. Of course, the observation of an internal distortion of the oxygen atoms at T_N (Ref. 5) gives indirect proof that quadrupolar effects are important, and the presence of quadrupoles at the U site is strongly inferred from the ²³⁵U NMR results.⁸ By using resonant x-ray scattering at the U M_4 resonance, where we probe the $5f$ valence states of UO_2 , we show conclusively the long-range nature of the $5f$ electric quadrupolar ordering. We further show that temperature dependence of this quadrupolar ordering is similar to that associated with the internal distortion of the oxygen cage (as expected), and demonstrate the difference between the electric quadrupolar ordering found in UO_2 and that reported for NpO_2 .¹⁸ We conclude by recalling studies of the mixed oxide systems $(\text{U}_{1-x}\text{Np}_x)\text{O}_2$ and speculate on the possible role of “quadrupolar frustration” in

explaining some of the unusual features of this phase diagram.

Experiments were carried out on the magnetic scattering beamline ID20 at the European Synchrotron Radiation Facility, Grenoble, France. The sample was mounted in a closed cycle refrigerator capable of reaching a base temperature of 12 K. This in turn was mounted within a 5-circle vertical diffractometer. Polarization analysis of the scattered beam was performed using the (111) reflection from a Au analyzer crystal for which the Bragg angle at the M_4 edge of uranium is close to Brewster’s angle.

The resonant x-ray scattering amplitude for an electric dipole (E1) transition can be written in a general form as

$$f_{E1}^{\text{xres}} = f_0 + if_1 + f_2, \quad (1)$$

where the terms f_n are given by the following equations

$$f_0 = \boldsymbol{\epsilon}_f \cdot \boldsymbol{\epsilon}_i [F_{11} + F_{1-1}],$$

$$f_1 = (\boldsymbol{\epsilon}_f \times \boldsymbol{\epsilon}_i) \cdot \hat{\mathbf{z}} [F_{11} - F_{1-1}],$$

$$f_2 = \boldsymbol{\epsilon}_f \cdot \tilde{\mathbf{T}} \cdot \boldsymbol{\epsilon}_i [2F_{10} - F_{11} - F_{1-1}], \quad (2)$$

where F_{1q} is the resonant energy factor,¹⁹ and $\hat{\mathbf{z}}$ is the direction of the magnetic moment. For σ incident polarization the terms in f_1 perform a rotation of the polarization of the incident x rays. However, terms in f_2 may or may not result in a rotation of the polarization.

The term in f_0 does not depend on multipole moments and can be neglected in this work. The term f_1 probes a tensor of rank 1, with odd time-reversal symmetry arising from a net spin polarization, a difference between overlap integrals, resonant energy, or lifetime for the two channels.¹⁹ The term f_2 probes a tensor of rank 2, even in time-reversal symmetry. This can arise from an asymmetry intrinsic to the crystal lattice (Templeton or anisotropic tensor susceptibility scattering²⁰) or it can be due to antiferro order of electric-quadrupole moments.

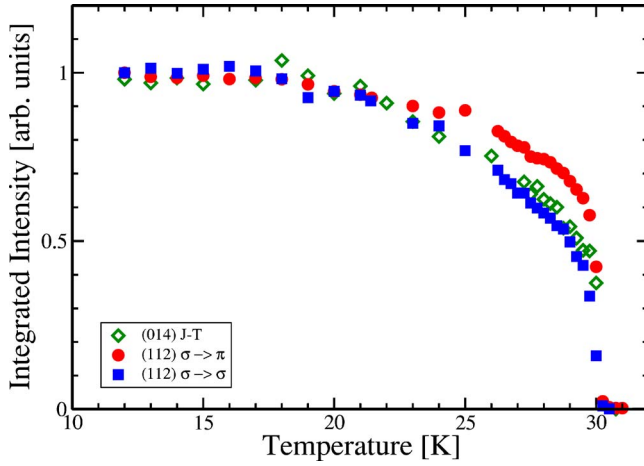


FIG. 1. (Color online) Temperature dependence of the integrated intensity of the (112) reflection in both $\sigma \rightarrow \pi$ (circles) and $\sigma \rightarrow \sigma$ (squares) polarization channels and the (014) Bragg reflection (diamonds, measured at 10 keV). These represent the magnetic dipole, electric-quadrupole order and Jahn-Teller distortion, respectively. Error bars are smaller than the data points.

For the case of electric-quadrupole moments, we first evaluate the quadrupolar operator for the $3\mathbf{k}$ structure of UO_2 given by

$$\mathbf{T}_{ij} = \mu_i \mu_j - \frac{1}{3} \delta_{ij} \sum_k (\mu_k \mu_k), \quad (3)$$

where μ is the principal axis of the electric quadrupole moment. From this we can obtain a “tensorial structure factor” \tilde{T}_Q , summing over all atoms within the unit cell. The scattered intensity is then deduced using Eq. (2) and given by

$$I(\mathbf{Q}) \propto |\boldsymbol{\epsilon}_f \cdot \tilde{T}_Q \cdot \boldsymbol{\epsilon}_i|^2, \quad (4)$$

where $\boldsymbol{\epsilon}_i$ and $\boldsymbol{\epsilon}_f$ are unit vectors along the incident and scattered x-ray electric field vectors, respectively. For the $3\mathbf{k}$ transverse structure of UO_2 there are two S domains which for scattering vectors of $\mathbf{Q}=(003)$ and $\mathbf{Q}=(112)$ yield tensors of the form

$$\tilde{T}^A = \begin{pmatrix} 0 & 0 & 0 \\ 0 & 0 & 1 \\ 0 & 1 & 0 \end{pmatrix}, \quad (5)$$

$$\tilde{T}^B = \begin{pmatrix} 0 & 0 & 1 \\ 0 & 0 & 0 \\ 1 & 0 & 0 \end{pmatrix}. \quad (6)$$

The reflections arising from these quadrupoles coincide with those due to magnetic dipole ordering. The experimental challenge is therefore to separate the two. This can be achieved by polarization analysis as for σ polarized incident x rays all scattering from the magnetic dipoles is $\sigma \rightarrow \pi$ with the signal from the electric-quadrupoles being scattered $\sigma \rightarrow \sigma$ and $\sigma \rightarrow \pi$. However, previous attempts to observe electric-quadrupolar scattering in UO_2 have failed for the following reason: It is usual in such systems to work in

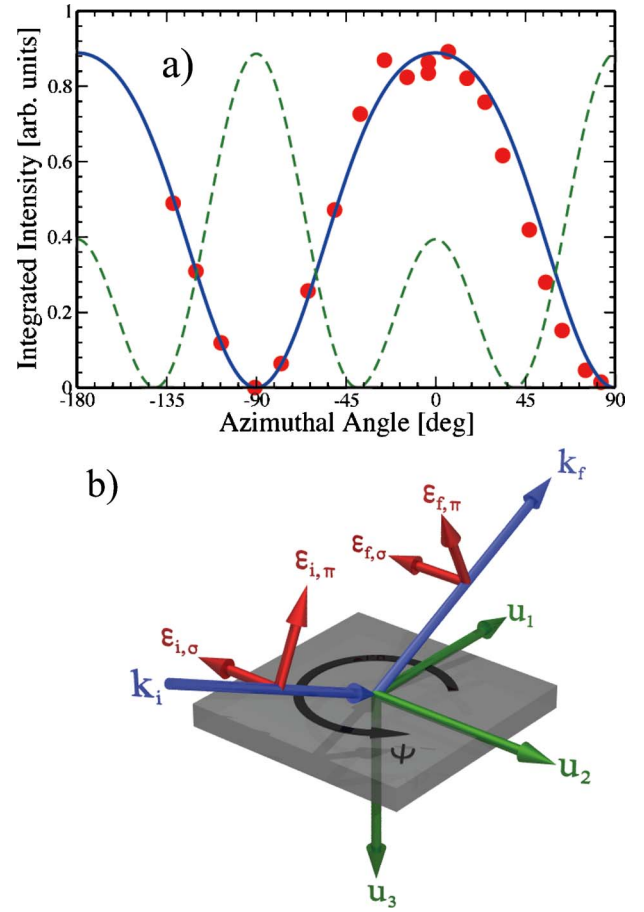


FIG. 2. (Color online) (a) The integrated intensity as a function of azimuthal angle Ψ for the (112) reflection measured in the $\sigma \rightarrow \sigma$ polarization channel (circles). The solid (dashed) line shows the expected azimuthal dependence for the transverse (longitudinal) model as described in the text. (b) Schematic representation of the scattering geometry used to measure the integrated intensity as a function of azimuthal angle. The arrows $\boldsymbol{\epsilon}_{i,\sigma}$ and $\boldsymbol{\epsilon}_{i,\pi}$ correspond to the electric field direction for the σ and π incident light, respectively. $\boldsymbol{\epsilon}_{f,\sigma}$ and $\boldsymbol{\epsilon}_{f,\pi}$ correspond to the electric field direction for the σ and π scattered light, respectively. The axes \mathbf{u}_1 , \mathbf{u}_2 , and \mathbf{u}_3 are consistent with those used by Hill and McMorro¹⁹ where \mathbf{u}_3 is antiparallel to \mathbf{Q} . Ψ denotes the azimuthal rotation.

specular geometry, which for a $[001]$ face crystal allows one to observe scattering at (001) and (003) at the $U M_4$ edge. In this configuration quadrupolar scattering from such reflections occurs only in the $\sigma \rightarrow \pi$ channel, and given the strong magnetic dipole scattering at the same wave vector it is therefore impossible to observe. On the other hand, by using an off-specular reflection, such as the (112) used in these measurements, the signal from the electric-quadrupolar scattering is partially $\sigma \rightarrow \sigma$ and therefore observable.

Figure 1 shows the integrated intensity as a function of temperature for the (014) and (112) reflections. Scattering from the (014) was collected at an incident photon energy of 10 keV, far away from the resonance condition and corresponds to the internal distortion of the oxygen sublattice.⁵ For the (112) an incident energy of 3.728 keV was used, corresponding to the $U M_4$ absorption edge. A strong reso-

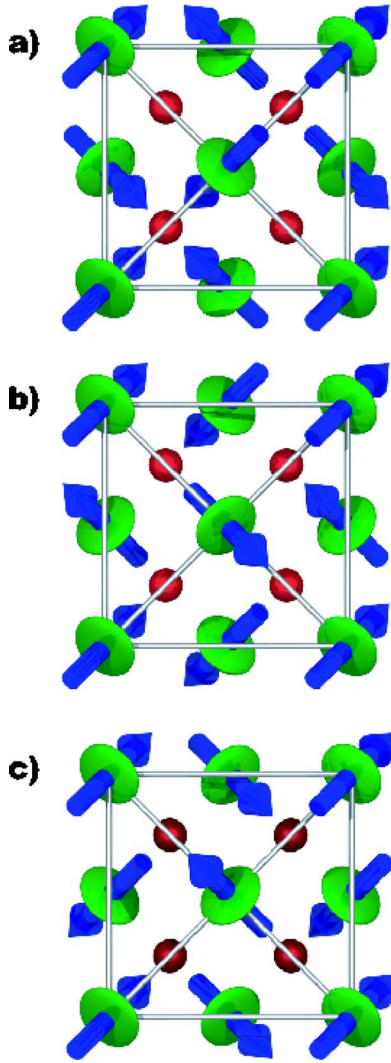


FIG. 3. (Color online) Schematic representation of the projection onto the a - b plane of the $3\mathbf{k}$ magnetic and electric-quadrupole ordering for the longitudinal (a) configuration and the two S -domains of the transverse configuration (b), (c). The magnetic (dipole) moments are represented by blue arrows whereas the electric-quadrupole moments are shown as the green ellipsoids. The red spheres represent oxygen atoms.

nant enhancement was observed upon changing the incident energy resulting in a line shape similar to that previously reported by Bernhoeft *et al.*²¹ for bulk scattering. Whereas the $\sigma \rightarrow \pi$ channel is dominated by the dipole order parameter, the intensity in the $\sigma \rightarrow \sigma$ channel arises solely from the electric quadrupole ordering. From Fig. 1 this order parameter (squares) follows the temperature dependence of the internal distortion of the oxygen atoms (diamonds). A close examination of the energy dependence of this quadrupole signal shows that it is centered about 2 eV below the position of the dipole resonance, and it has an approximate Lorentzian squared shape with a narrow full width at half maximum of ≈ 3 eV. This is similar to that found in NpO_2 (Ref. 22) and also in the mixed compound $\text{U}_{0.75}\text{Np}_{0.25}\text{O}_2$ for the quadrupole signals.²³ From these data it is apparent that the electric quadrupolar order parameter follows the tem-

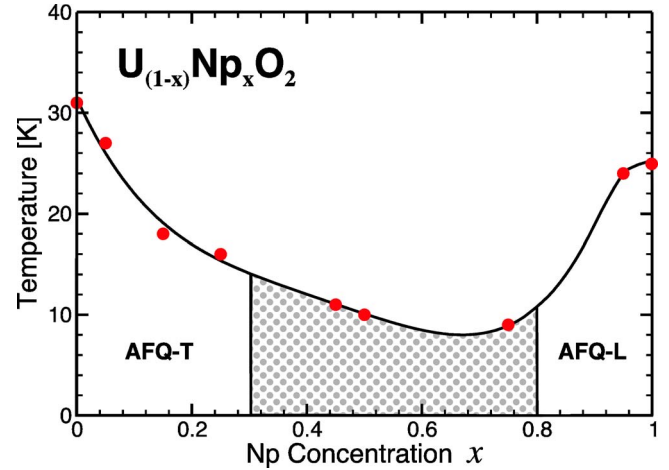


FIG. 4. (Color online) Suggested phase diagram for the $\text{U}_{(1-x)}\text{Np}_x\text{O}_2$ system as derived from various measurements. The known regions of antiferroquadrupolar order are marked by AFQ-T (AFQ-L) for the transverse (longitudinal) case. The shaded region in the center denotes the frustrated region of the phase diagram. (See text for details.)

perature dependence of the internal distortion.

As the sample is rotated around the scattering vector (azimuthal rotation) [cf. Fig. 2(b)] the intensity of the superlattice peak exhibits a characteristic oscillation due to the relative rotation of the electric field vector with respect to the crystal lattice. It is this oscillation which enables us to determine the origin of the observed signal. Figure 2 shows the integrated intensity for the (112) reflection as a function of the azimuthal angle (Ψ) in the $\sigma \rightarrow \sigma$ polarization channel. The data were collected at a temperature of 12 K. The origin of Ψ corresponds to the condition when the $[\bar{1}10]$ direction lies within the scattering plane. For this reflection, the azimuthal dependence of the intensity is given by an incoherent addition of the two transverse S domains (see Fig. 3),

$$I_{(112)} = A[|\boldsymbol{\epsilon}_f \cdot \tilde{T}_A \cdot \boldsymbol{\epsilon}_i|^2 + |\boldsymbol{\epsilon}_f \cdot \tilde{T}_B \cdot \boldsymbol{\epsilon}_i|^2], \quad (7)$$

where \tilde{T}_A and \tilde{T}_B are the scattering tensors given in Eqs. (5) and (6), respectively. This can be evaluated to give

$$I_{(112)} = \frac{4}{3}A \cos^2 \Psi \left[1 - \frac{1}{3} \cos^2 \Psi \right]. \quad (8)$$

A comparison between Eq. (8) and the experimental data is shown in Fig. 2. The dashed line in Fig. 2 corresponds to the case of a longitudinal structure. This shows unambiguously that, with respect to the propagation vector, the orientation of the electric quadrupoles in UO_2 is transverse contrary to the case of NpO_2 in which a longitudinal orientation is found.^{22,24} Interestingly, because of the crystal-field ground state²⁵ there is no magnetic-dipole order in NpO_2 . However, both UO_2 and NpO_2 are now established to have electric-quadrupole ordering at low temperature, and in both materials the ordering is $3\mathbf{k}$ in nature (Refs. 6–8, 22, 24, and 26).

Finally, we turn to the intriguing question of the magnetic behavior of the solid solutions $(\text{U}_{1-x}\text{Np}_x)\text{O}_2$ that was re-

ported some years ago, as well as some recent measurements on single crystals at ITU, Karlsruhe. We show in Fig. 4 the experimental points determining the “ordering” temperatures as a function of the Np concentration, x . Since the ordering interactions in both UO_2 ($x=0$) and NpO_2 ($x=1$) lead to $T_0 \sim 25$ K the sudden drop in T_0 on dilution at either end is surprising, as we would naively expect a Vegard-type law for T_0 . Moreover, for the region $\sim 0.3 < x < \sim 0.8$, neutron and Mössbauer experiments show a surprising short-range ordering²⁷ with propagation wave vector close to $\langle \frac{1}{2} \frac{1}{2} \frac{1}{2} \rangle$ that is not yet well characterized or understood.

The experiments reported in this paper, as well as in earlier works,^{22–24} show that the important parameter across this phase diagram for all x is antiferroquadrupolar (AFQ) ordering of the electric quadrupoles. For small x , as shown in Fig. 3, the AFQ ordering is transverse, whereas for large x near NpO_2 (Refs. 22 and 24) the ordering is longitudinal. In both cases the same wave vector $\mathbf{q}_{AFQ} = \langle 001 \rangle$ is observed. Our

suggestion, therefore, is that over the large intermediate range of x (shown by the shaded region in Fig. 4) a state of frustrated quadrupolar ordering exists, where neither the AFQ-transverse (AFQ-T) nor AFQ-longitudinal (AFQ-L) order can dominate, leading to short-range ordering of the quadrupoles and associated dipole moments. As electric quadrupoles are a secondary order parameter in these compounds, the frustration could reflect a competition between Np-Np octupolar interactions favoring longitudinal AFQ and U-Np and U-U dipole interactions favoring transverse AFQ. Further experiments in this interesting region are planned with XRS and other techniques such as NMR.

S.B.W. would like to acknowledge support from the European Commission in the framework of the “Training and Mobility of Researchers” program. G.H.L. thanks Russ Walstedt of JAERI (Japan) for many interesting discussions about actinide oxides.

-
- ¹B. T. M. Willis and R. I. Taylor, *Phys. Lett.* **17**, 188 (1965).
²B. C. Frazer *et al.*, *Phys. Rev.* **140**, A1448 (1965).
³O. G. Brandt and C. T. Walker, *Phys. Rev.* **170**, 528 (1968).
⁴R. A. Cowley and G. Dolling, *Phys. Rev. Lett.* **16**, 683 (1966).
⁵J. Faber and G. H. Lander, *Phys. Rev. B* **14**, 1151 (1976).
⁶P. Burlet *et al.*, *J. Less-Common Met.* **121**, 121 (1986).
⁷G. Amoretti, A. Blaise, R. Caciuffo, J. M. Fournier, M. T. Hutchings, R. Osborn, and A. D. Taylor, *Phys. Rev. B* **40**, 1856 (1989).
⁸K. Ikushima, S. Tsutsui, Y. Haga, H. Yasuoka, R. E. Walstedt, N. M. Masaki, A. Nakamura, S. Nasu, and Y. Onuski, *Phys. Rev. B* **63**, 104404 (2001).
⁹S. J. Allen, *Phys. Rev.* **166**, 530 (1968).
¹⁰S. J. Allen, *Phys. Rev.* **167**, 492 (1968).
¹¹K. Sasaki and Y. Obata, *J. Phys. Soc. Jpn.* **28**, 1157 (1970).
¹²R. Siemann and B. R. Cooper, *Phys. Rev. B* **20**, 2869 (1979).
¹³G. Solt and P. Erdős, *Phys. Rev. B* **22**, 4718 (1980).
¹⁴K. N. Kudin, G. E. Scuseria, and R. L. Martin, *Phys. Rev. Lett.* **89**, 266402 (2002).
¹⁵R. Laskowski, G. K. H. Madsen, P. Blaha, and K. Schwarz, *Phys. Rev. B* **69**, 140408 (2004).
¹⁶N. Magnani, P. Santini, G. Amoretti, and R. Caciuffo, *Phys. Rev. B* **71**, 054405 (2005).
¹⁷D. Ippolito, L. Martinelli, and G. Bevilacqua, *Phys. Rev. B* **71**, 064419 (2005).
¹⁸A. V. Nikolaev and K. H. Michel, *Phys. Rev. B* **68**, 054112 (2003).
¹⁹J. P. Hill and D. F. McMorrow, *Acta Crystallogr., Sect. A: Found. Crystallogr.* **52**, 236 (1996), and references therein.
²⁰D. Templeton and L. Templeton, *Acta Crystallogr., Sect. A: Found. Crystallogr.* **41**, 133 (1985).
²¹N. Bernhoeft, A. Hiess, S. Langridge, A. Stunault, D. Wermeille, C. Vettier, G. H. Lander, M. Huth, M. Jourdan, and H. Adrian, *Phys. Rev. Lett.* **81**, 3419 (1998).
²²J. A. Paixao, C. Detlefs, M. J. Longfield, R. Caciuffo, P. Santini, N. Bernhoeft, J. Rebizant, and G. H. Lander, *Phys. Rev. Lett.* **89**, 187202 (2002).
²³S. B. Wilkins, J. A. Paixao, R. Caciuffo, P. Javorsky, F. Wastin, J. Rebizant, C. Detlefs, N. Bernhoeft, P. Santini, and G. H. Lander, *Phys. Rev. B* **70**, 214402 (2004).
²⁴R. Caciuffo, J. A. Paixão, C. Detlefs, M. J. Longfield, P. Santini, N. Bernhoeft, J. Rebizant, and G. H. Lander, *J. Phys.: Condens. Matter* **15**, S2287 (2003).
²⁵N. Magnani, P. Santini, G. Amoretti, R. Caciuffo, P. Javorsky, F. Wastin, J. Rebizant, and G. H. Lander, *Physica B* **359-361**, 1087 (2005).
²⁶Y. Tokunaga, Y. Homma, S. Kambe, D. Aoki, H. Sakai, E. Yamamoto, A. Nakamura, Y. Shiokawa, R. E. Walstedt, and H. Yasuoka, *Phys. Rev. Lett.* **94**, 137209 (2005).
²⁷A. Boeuf *et al.*, *Europhys. Lett.* **3**, 221 (1987), and references therein.